Available online at www.sciencedirect.com
ScienceDirect
Composites Science and Technology 67 (2007) 829–839
COMPOSITES SCIENCE AND TECHNOLOGY
www.elsevier.com/locate/compscitech

Viscoelastic behavior and electrical properties of flexible nanofiber filled polymer nanocomposites. Influence of processing conditions

Florent Dalmas [a,b], Jean-Yves Cavaillé [a], Catherine Gauthier [a], Laurent Chazeau [a,*], Rémy Dendievel [b]

[a] *Groupe d'Etude de Métallurgie Physique et de Physique des Matériaux (GEMPPM), INSA de Lyon, bât. B. Pascal, 7, av. J. Capelle, 69621 Villeurbanne cedex, France*

[b] *Génie Physique et Mécanique des Matériaux (GPM2), INP Grenoble, ENSPG, BP46, 38402 St Martin d'Hères, France*

Received 31 October 2005; accepted 24 January 2006
Available online 12 October 2006

Abstract

Two different types of high aspect ratio flexible nanofibers, cellulose nanofibrils and carbon nanotubes, were dispersed in an amorphous thermoplastic polymer matrix. The mechanical and (in the case of carbon nanotubes filled composites) electrical properties of these composites were investigated. Dynamic mechanical analysis highlighted the influence of entanglements between fibers and of fiber/fiber contact properties on the composite mechanical reinforcement in the rubbery state. In the case of cellulose filled nanocomposites a large mechanical reinforcement effect was observed. This effect was explained by the formation of a rigid nanofibril network linked by strong hydrogen bonds. The formation of this network was assumed to be governed by a percolation mechanism. Conversely, when such bonds between cellulose fibrils were prevented by the process, a lower mechanical reinforcement is observed and can be modeled by a classical mean field approach. On the other hand, both types of composites filled with carbon nanotubes (where no strong interactions are possible) highlighted the fact that entanglements are responsible for a strong increase in thermo-mechanical stability but do not influence the mechanical reinforcement. However, carbon nanotubes are good conductive objects and for such nanocomposites, electrical percolation properties were found. The influence of the process on these electrical properties was highlighted and discussed in term of modification of tube–tube contact electrical properties.

Keywords: A. Polymer-matrix composites; A. Nanostructures; B. Mechanical properties; B. Electrical properties

1. Introduction

Made up of nanometric particles (nanofillers) dispersed in a polymer matrix, nanocomposite materials have been widely studied in the past 20 years. The mechanical reinforcement effect of these nanofillers were soon highlighted. In the particular case of polymer reinforced with rigid nanofillers, various parameters seem to be of importance in characterizing the fillers: geometrical factors such as the shape, the size, and the aspect ratio; intrinsic mechanical characteristics such as the modulus or the flexibility; surface properties such as specific surface area and surface treatment [1]. The type of polymer matrix used and the possible effects of nanofillers on its microstructure and its intrinsic properties is also an essential parameter ruling the composite properties. Indeed, the presence of nanofillers could modify the crystallinity of a semi-crystalline matrix, or the cross-linking in a thermoset matrix. Thus, the fundamental understanding of the relations between the microstructure and the mechanical properties of nanocomposites is strongly made easier by using simple amorphous thermoplastic matrices.

* Corresponding author. Tel.: +33 4 72 43 61 30; fax: +33 4 72 43 85 28.
E-mail address: laurent.chazeau@insa-lyon.fr (L. Chazeau).

0266-3538/$ - see front matter © 2006 Elsevier Ltd. All rights reserved.
doi:10.1016/j.compscitech.2006.01.030

High aspect ratio fillers are of particular interest because of their high specific surface area. In the case of fibrous nanofillers, previous experimental and theoretical studies have essentially focused on rod-like nanofibers (cf: the work of Favier et al. on cellulose whiskers as fillers in a polymer matrix [2,3]). However, very high aspect ratio nanofibers display good flexibility properties. Dispersed in polymer matrices, they will create a complex entangled microstructure. The influence of the entanglement rate, the tortuosity of the fillers, their intrinsic properties and the filler–filler interactions on the composite macroscopical properties is not completely understood yet. The need for experimental study and theoretical modeling of model systems have motivated the present work.

In order to understand the effect of interactions between nanofibers, two different types of flexible nanofibers were used: cellulose nanofibrils and carbon nanotubes. Moreover, by using two different processing conditions, entanglements and contacts between nanofibers could be modified.

The cellulose is a semi-crystalline biopolymer, naturally synthesized as nanofibrils, which constitute the rigid skeleton of numerous species such as plants, some alga or mushrooms and amoebae [4]. Eichhorn and Young [5] have measured by in situ Raman spectroscopy a value of 25 GPa for the longitudinal Young's modulus of cellulose fibrils. Because of their interesting mechanical properties and the progress made for their extraction and their individualization from natural materials [6], cellulose nanofibrils were recently studied as fillers in polymer matrices [7,8].

Concerning carbon nanotubes, papers related to their use in nanocomposite materials are more and more numerous since their discovery by Ijima in 1991 [9]. Even if experimental studies [10] and theoretical modeling [11] have demonstrated high Young's modulus (of the order of magnitude of 1 TPa) and stiffness of carbon nanotubes, their real efficiency as a mean to increase the mechanical reinforcement in polymer matrices is still an open question as suggested by the diversity of the results found in the literature [12–16]. In addition to their outstanding mechanical properties, carbon nanotubes are good electrical conductive objects [17]. Dispersed in an insulating matrix, they allow the material to be conductive above a certain nanotube content, called the electrical percolation threshold; but, here again, results in the literature are very scattered [18–21].

The aim of this study is thus to check the efficiency of multi-walled carbon nanotubes (MWNTs) – which were chosen because of their weak interactions (contrary to single-walled carbon nanotubes which form bundles, difficult to disintegrate) – as fillers in a soft thermoplastic matrix and to compare it with that of cellulose nanofibrils. In order to realize this study, model systems were elaborated and tested. Stable suspensions of MWNTs and nanofibrils were, first, mixed with an aqueous emulsion of polymer particles, i.e. a latex. In order to produce composite films, two different processing conditions were then used. We report here dynamic mechanical analysis measurements and electrical characterization of these materials.

2. Experimental

2.1. Characterization

A drop of diluted suspension of MWNTs in ethanol or cellulose nanofibrils in water was deposited on amorphous carbon-coated TEM grids and then observed at room temperature using a JEOL 200CX transmission electron microscope (TEM).

In order to check the nanocomposites homogeneity (i.e. the dispersion of the nanofillers in the matrix), conventional TEM observations were also performed on composite materials. The samples were cut by cryo-ultramicrotomy using a Ultracut Reichert S. The temperature of the sample was set to −20 °C and the speed of the glass knife was 4 mm s^{-1}. The thin sections of about 60 nm thick were dry-collected and were placed on a 400-mesh copper grid.

Differential scanning calorimetry (DSC) analysis was performed on a Perkin–Elmer Pyris Diamond apparatus with a heating rate of 10 K/min. The glass transition temperature, T_g, mentioned in the text refers to the temperature of the inflexion point on DSC data.

For the mechanical characterization, dynamic mechanical analysis (DMA) measurements were performed in torsion mode at a fixed frequency (0.1 Hz) from 200 K to 450 K with a heating rate of 1 K/min. The storage (G') and the loss (G'') moduli of the complex shear modulus (G^*) and the loss factor $\tan(\delta)$ (G''/G') were measured as a function of temperature. Sample dimensions were about $10 \times 3 \times 0.6$ mm^3. The main relaxation temperature T_α is defined here as the temperature where the maximum of $\tan(\delta)$ is reached.

Electrical conductivity measurements were carried out. Parallelepipedic samples (around $5 \times 15 \times 0.7$ mm^3) were coated at their ends with a silver paint to ensure a good electrical contact with the electrodes. AC complex electrical conductivity measurements were performed at room temperature for several frequencies ranging from 10 mHz to 1 MHz using a Solartron 1226 bridge with a low applied field of about 1 V cm^{-1}. The complex admittance Y^* was recorded versus time. From this admittance, the complex conductivity σ_e^* can be deduced.

2.2. Materials

2.2.1. Cellulose nanofibrils

These were obtained from sugar beet pulp at the Centre de Recherche sur les Macromolécules Végétales (CERMAV, CNRS, B.P. 53, 38041 Grenoble Cedex, France). The chemical treatment used is described by Dinand et al. [6]. This treatment allows to obtain a final aqueous suspension of cellulose nanofibrils which does not sediment or flocculate. A TEM observation of this cellulosic fibrils is

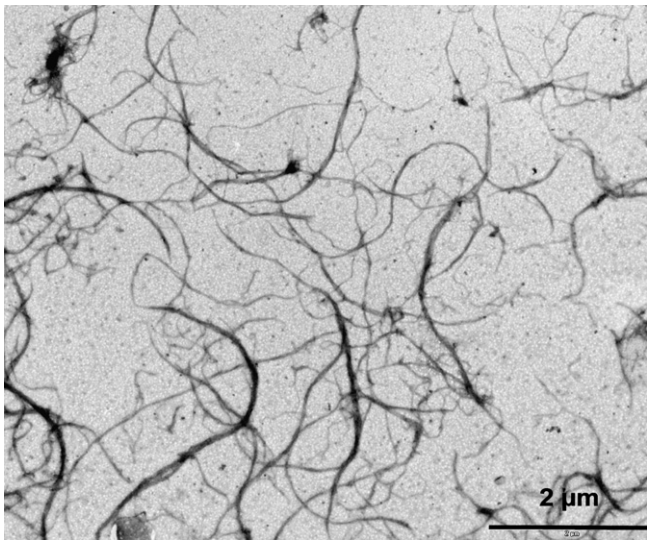

Fig. 1. TEM observation of cellulose nanofibrils extracted from sugar beet.

presented in Fig. 1. Because of cellulose degradation under the electron beam, TEM high magnification observations and thus the observation of individual nanofibrils are really difficult to run. Nevertheless, one can observe in Fig. 1 that cellulose nanofibrils are arranged in bundles of 10–50 nm width. The cellulose relative density is 1.58 g cm^{-3}.

2.2.2. Multi-walled carbon nanotubes

These were synthesized at Ecole Polytechnique Fédérale de Lausanne (EPFL) from the catalytic decomposition of acetylene at 720 °C on supported cobalt/iron catalyst as already described [22]. For purification, raw MWNTs sample was sonicated in 30% HNO_3 for 3 h then filtered and washed with distilled water and finally dried at 120 °C. As shown in Fig. 2, the purified multi-walled carbon nanotubes used in this study are pure, very long (mean length around 8 μm), flexible and entangled. Couteau and co-workers [22] previously showed by energy dispersive X-ray (EDX) analysis that with this purification process

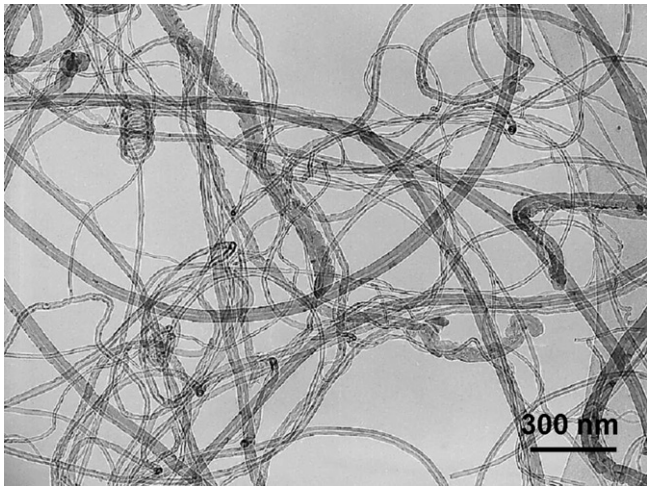

Fig. 2. TEM observation of multi-walled carbon nanotubes after purification in nitric acid.

the Fe (K_α 6.4 eV and K_β 7.06 eV) and Co (K_α 6.93 eV and K_β 7.65 eV) peaks are drastically reduced in the purified sample. This means that the metallic catalysts are mainly removed by the purification step. Image analysis made on several TEM pictures gives a diameter distribution between 8 nm and 105 nm with a mean value around 32 nm. The relative density of MWNTs can be estimated to 2 g cm^{-3} by taking into account the volume of graphite (relative density 2.2 g cm^{-3}) in a nanotube.

The purified nanotubes were then dispersed in a distilled water solution of 1.2 g L^{-1} sodium dodecylbenzene sulfonate (SDBS: $C_{18}H_{29}SO_3Na$) surfactant using a sonication step for 10 min with 20 mL suspension volumes, using a Branson Sonifier with a 13 mm probe tip at 20 KHz and a power source of 25 W. Several weight ratios of nanotubes to surfactant were investigated for solution stability and an optimum ratio of five (5:1) was chosen to obtain an aqueous suspension stable for at least 3 weeks. This weight ratio corresponds to six surfactant molecules per nm^2 of available nanotube surface (calculation made with an average tube diameter of 32 nm), or in other words a surface available for each molecule of 14 $Å^2$, which seems reasonable. The quality and the homogeneity of this MWNTs aqueous suspension was established by new environmental scanning electron microscopy observations. Bogner et al. [23] have developed a new device which allowed the observation of aqueous dispersion in transmission. Latex and carbon nanotubes dispersion previously mentioned were observed and found to present a good state of dispersion without aggregates.

2.2.3. The latex matrix

This was prepared by emulsion copolymerization of styrene (35 wt%) and butyl acrylate (65 wt%) at the LCPP (Laboratoire de Chimie et Procédés de Polymérisation, UMR CNRS 140-CPE Lyon, BP 2077, 69616 Villeurbanne Cedex, France). The polymerization occurs in a miscellar aqueous solution of a surfactant mixture: an anionic ($C_{12}H_{25}O(CH_2$-$CH_2O)_4SO_3Na$) and a non-ionic ($C_{12}H_{25}O(CH_2CH_2O)_{19}H$). A surfactant-stabilized aqueous suspension of poly(styrene-co-butyl acrylate), P(S-BuA), with a relative density of 1.07 g cm^{-3} is obtained containing 43 wt% of spherical polymer particles with an average diameter of (145 ± 11) nm (determined by light scattering). The glass transition temperature of P(S-BuA) was determined by differential scanning calorimetry and found to be 266 K.

2.2.4. Composite processing

The latex was first stirred with the stable aqueous suspensions of nanofillers. Two methods were then used for the composite processing. The mixture was either cast in an aluminum mold with a teflon coating and put in a drying oven at 35 °C under vacuum for five days to allow slow water evaporation and film formation (i.e. polymer particles coalescence). So-called evaporated films (or materials E) were obtained. For the second process used to elaborate composites, the suspension mixture was first freeze-dried to

allow water sublimation, and a compact soft powder was obtained. This powder was then pressed at 100 °C for 5 min under 1 MPa after 45 min of thermal stabilization without pressure. This second type of nanocomposite materials is referred as FP materials.

Samples reinforced with nanofillers contents of up to 6 vol% for cellulosic nanofibrils and up to 3 vol% for MWNTs fillers, were processed.

3. Results and discussion

3.1. Microstructural characterization

The good level of dispersion of nanofillers within the P(S-BuA) matrix can be seen on Fig. 3 which shows an example of TEM observations on composites. Indeed, no aggregate can be observed and both nanotubes and nanofibrils seem to be isolated and homogeneously distributed. It is remarkable that on a composite microsection, nanofibers seem to be shorter and less entangled than what they are really in the corresponding macroscopic sample, because of the small observed thickness.

3.2. Glass transition temperature

DSC analysis highlighted the influence of processing conditions and filler content on the P(S-BuA) glass transition temperature, T_g. Indeed, FP materials systematically present T_g about 4 K lower than those of E materials. As an example, the pure P(S-BuA) matrix has a T_g of 266 K when evaporated and of 262 K when freeze-dried. This observation suggested a strong influence of the processing on the surfactant organization within the polymer. Indeed, the surfactant used here is known to have a plasticizing effect on latex films. After the latex film formation by slow evaporation, the surfactant molecules can be either solubilized in the polymer, dispersed as aggregates within the film, or segregated at the film surface or at the film-substrate interface [24]. The freeze-drying step followed by hot-pressing could strongly limit the eventual segregation and migration of surfactant molecules. Thus, the residual amount of surfactant in the film would be higher. A higher amount of surfactant solubilized in the polymer would lead to a lower T_g because of the plasticizing effect. Moreover, the presence of nanofillers in the latex may modify the equilibrium established between surfactant molecules solubilized in the matrix and those segregated or adsorbed on filler surface. Indeed, for each process and for both kind of fillers, T_g increases with the filler volume fraction. Nowadays, this problem of surfactant arrangement in latex films is still the object of numerous scientific publications [25] and is far from being completely understood. In the continuation of the present paper, in order to be free of this problem in the analysis of the results, the latter will be presented as a function of the ratio T/T_α, with T_α the main relaxation temperature.

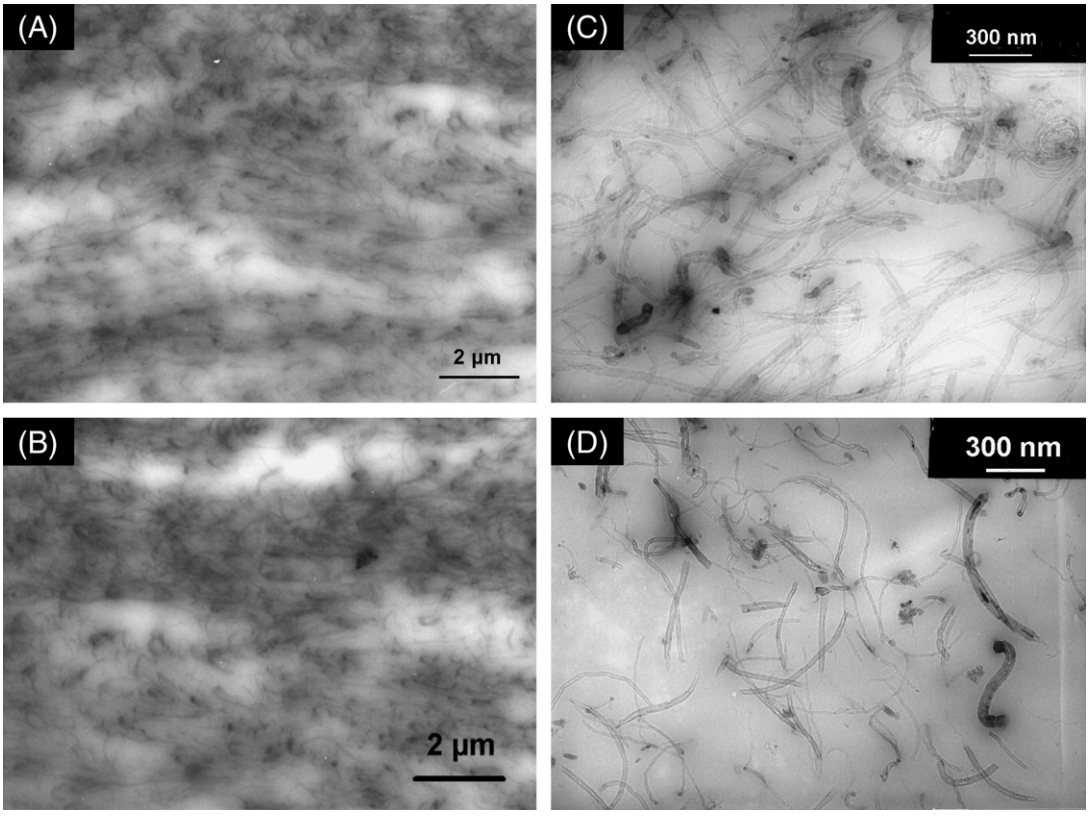

Fig. 3. Low magnification TEM micrographs of microsections from a P(S-BuA) film filled with 4 vol% of cellulose nanofibrils E (A) or FP (B), and with 3 vol% of MWNTs E (C) or FP (D).

3.3. Viscoelastic behavior

3.3.1. DMA results

The storage modulus G' (which is indicative of the elastic behavior of the polymer) determined by DMA measurements for the pure P(S-BuA) matrix and related composite materials filled with 1.5 and 3 vol% of carbon nanotubes are plotted versus the normalized temperature in Fig. 4. The unfilled P(S-BuA) matrix displays classical behavior of amorphous thermoplastic polymer; well below T_α (281 K for the E matrix), the polymer is in the glassy state with a modulus roughly constant (around 1 GPa). When T_α is reached, a strong decrease of the elastic shear modulus (by more than 3 decades) occurs, corresponding to a peak of the loss factor tan(δ). Above T_α the material is in the rubbery state until it starts to flow (here at around 350 K) and to behave as a viscous fluid and, then the experimental apparatus fails.

When this matrix is filled with MWNTs, and whatever the processing condition used, a mechanical reinforcement effect is observed, increasing with the nanotube content. Below T_α, the increase in the modulus with nanotube content is moderate but the nanotubes efficiency above T_α is higher. Moreover, both 1.5 and 3 vol% MWNTs filled E systems display a large rubbery plateau where the modulus is almost constant with the temperature. This strong increase in composite thermo-mechanical stability cannot be only understood by interactions between the polymer chains and the nanotube surface, but the formation of a percolating entangled nanotube network within the material has to be taken into account. Entanglements between tubes explain the elastic modulus measured in this large temperature range (where the pure matrix behaves as a viscous fluid). The Fig. 5 shows the difference between a simple contact and an entangled contact between two fibers. Entanglements within a fibrous structure are indeed responsible for the elastic response of this structure (like in glass wool for example).

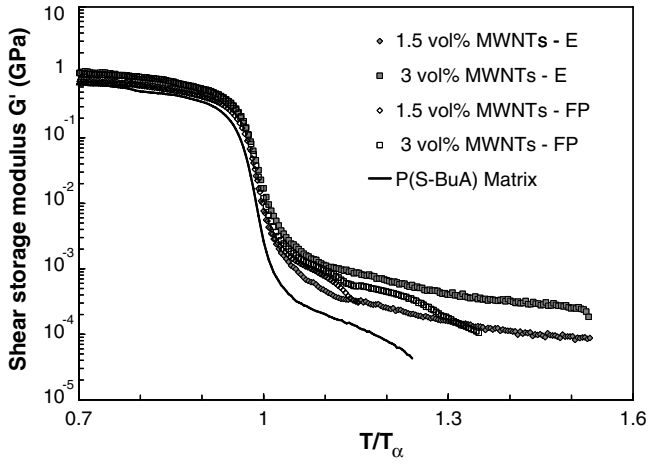

Fig. 4. Storage shear modulus G' as a function of normalized temperature for the unfilled P(S-BuA) matrix and related composites filled with multi-walled carbon nanotubes.

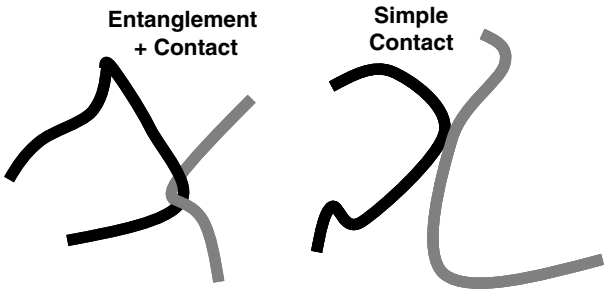

Fig. 5. Representation of an entanglement leading to a contact between two fibers; and of a simple fiber/fiber contact.

FP composites with the same nanotube contents do not display such a strong increase in flow temperature. Indeed, nearly the same mechanical reinforcement is measured but the FP materials rapidly flow. A scheme is proposed in Fig. 6 to explain this effect of processing conditions on thermo-mechanical results. During the slow evaporation, because of Brownian motions in the suspension (whose viscosity remains low, up to the end of the process when the particle concentration becomes very high), the rearrangement of the nanofibers is possible. The resulting structure (after the coalescence of polymer particles) is completely relaxed and entanglements between the long and flexible nanofibers are then created. Conversely, during the FP process, the particle arrangement in the suspension is first frozen, and then, during the hot-pressing, because of the melted polymer viscosity, the nanofiber rearrangements are strongly limited. In the resulting structure, the nanofibers are more isolated from each other (cf: Fig. 6), fiber/fiber contacts are mainly simple contacts, and very few entanglements are created. This latter FP microstructure will lead to a weak thermo-mechanical stability. Indeed, when the polymer is viscous, as only few entanglements exist between nanotubes, the composite flow (at a lightly higher temperature because of interactions between polymer chains and nanotubes).

However, entanglements between nanotubes appear to have a low effect on the mechanical reinforcement. Thus, the increase in modulus is mainly due to stress transfer between matrix and nanotubes.

Fig. 7 presents DMA results obtained on cellulose nanofibrils filled composites. Here again, an increase of the flow temperature is observed in both E and FP materials. This delay of the material flowing is due to the interactions between the polymer chains and the nanofibrils surface. For E materials, the slope value (in absolute value) of the rubber plateau is slightly lower for the composites than for the unfilled matrix. This can be explained by an increasing contrast between the fibrils and the matrix modulus when the matrix modulus decreases. Indeed, this contrast is known to have a great influence on the reinforcement effect of the fillers. For E composites, the modulus in the rubbery state appears constant with the temperature for

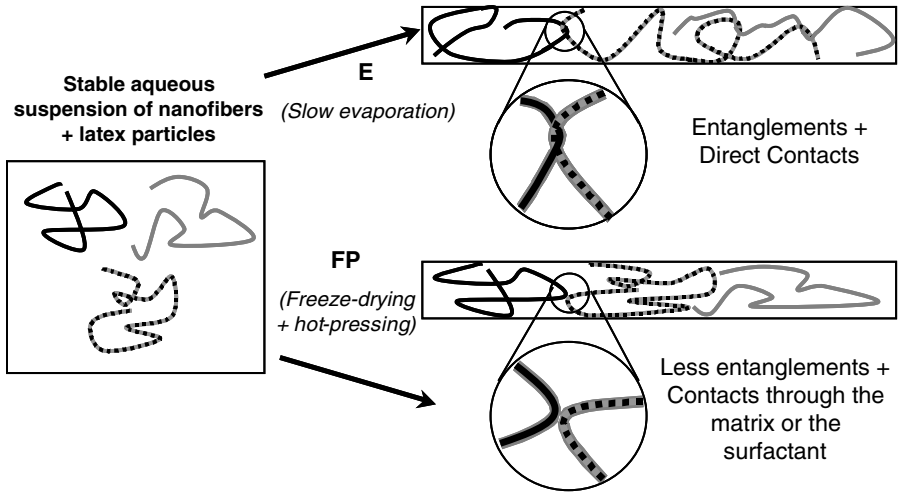

Fig. 6. Schematic representation of the possible influence of processing conditions on entanglements and contacts between nanofibers.

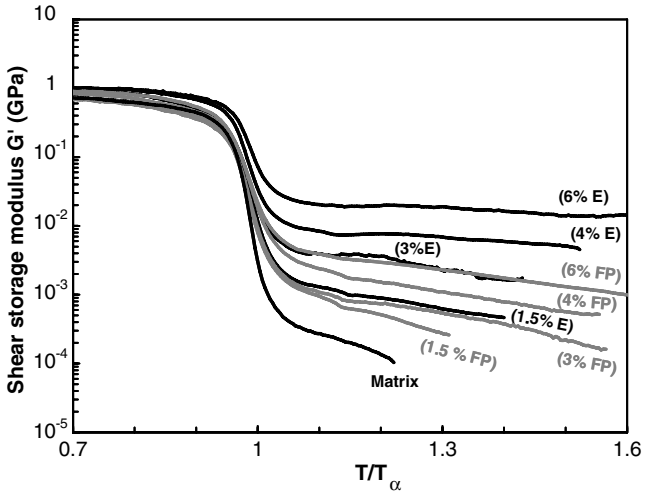

Fig. 7. Storage shear modulus G' as a function of normalized temperature for the unfilled P(S-BuA) matrix and related composites filled with cellulose nanofibrils. Black lines and gray lines are for E and FP materials, respectively. Cellulose contents are given in vol%.

nanofibril content higher or equal to 3 vol%. As supposed previously for MWNTs filled composites, such a long plateau results from a percolating filler network formed within the matrix. Nevertheless, the level of this modulus plateau is strongly higher for E cellulose filled composites than for E MWNTs filled ones with the same filler contents. This means that the rigidity of the nanofibril network is higher than that of the nanotube network. The rigidity of this cellulosic network is actually due to the strong hydrogen bonds which can be created between nanofibrils because of the high number of hydroxyl groups on their surface [2]. Up to the degradation of the cellulose (which occurs for a temperature around 500 K), the composite modulus is governed by this network rigidity. Thus, in this case, the mechanical reinforcement observed here is more the result of strong links between nanofibers than an entanglement effect.

Conversely, compared to E materials, cellulose filled FP materials present a mechanical reinforcement less important and the difference between the slopes on the rubbery plateau is smaller for such materials. This excludes the presence of this rigid nanofibril network in such materials. Thus, the FP process not only prevents entanglements creation between nanofibers (scheme proposed in Fig. 6) but also, the fiber/fiber contacts created during this process cannot be considered as direct contacts but are made through a certain amount of polymer matrix (or maybe surfactant in the case of nanotube fillers). This observation is confirmed by the previous results of Favier et al. [2] which established the fact that the freeze-drying process prevents or, at least, limits the creation of hydrogen bonds between cellulose nanofillers. Consequently, the modulus of the FP composites is only due to stress transfer between the matrix and the nanofibrils and decreases with the temperature.

3.3.2. Mechanical modeling

Various models exist for the mechanical properties of heterogeneous materials. Our approach uses the Halpin–Tsai semi-empirical equation [26] that describes the modulus of an aligned short-fiber composite, M_c, by:

$$\frac{M_c}{M_m} = \frac{1 + \xi\eta\psi}{1 - \eta\psi} \tag{1}$$

where η is given by:

$$\eta = \frac{(M_f/M_m) - 1}{(M_f/M_m) + \xi} \tag{2}$$

where ψ is the volume fraction of fibers, M_f the fibers modulus, M_m the matrix modulus and ξ is a factor that depends on the shape of the filler particle and on the type of modulus M to be calculated. The ply shear modulus G can be predicted with ξ equal to 1, the longitudinal modulus E_{11} with ξ equal to 2 L/d (L and d are the fiber length and diameter, respectively) and the in-plane moduli E_{22} or E_{33}

with ξ equal to 2 [27]. As shown by Van Es [28], the laminate theory can be used to calculate the isotropic three-dimensional modulus, as follows:

$$E_{3D} = 0.184E_{\parallel} + 0.816E_{\perp} \quad (3)$$

where $E_{||}$ and $E_{\perp}$ are, respectively, the parallel and perpendicular moduli calculated for a unidirectional fiber ply (given by the Halpin–Tsai formula Eq. (1)).

In order to fit Eq. (3) to the experimental data for cellulose filled composites in the rubbery state, we used for the fibers a longitudinal modulus E_{f11} equal to 30 GPa and transversal moduli E_{f22} and E_{f33} equal to 15 GPa. These values were taken from the literature on cellulose fibrils [29]. In the rubbery state, the fiber aspect ratio is the main parameter influencing the reinforcement level. To well fit the modulus of the cellulose filled composites above T_α, an aspect ratio (ratio of the length to the diameter of the fiber) of 312 is used. Even if high resolution electron microscopy on cellulosic objects is impossible, this aspect ratio value seems to be reasonable and is comparable to the estimation made by E. Dinand [30]. Fig. 8 shows the result of this model compared to the experimental data when the composites are in the rubbery state ($T/T_\alpha = 1.15$) for different fiber contents. It can be observed that the mechanical reinforcement for cellulose filled FP materials can be well modeled by the isotropic Halpin–Kardos calculation. Indeed such a model takes into account the modulus of each phase, as well as the geometry of the particles, but the particles are assumed to have no interaction among each other. This is consistent with the assumption of no strong hydrogen bonds between nanofibrils in FP materials. And, as expected, the mechanical reinforcement for E cellulose filled materials cannot be described by this mean field approach because of the presence of these strong filler–filler interactions.

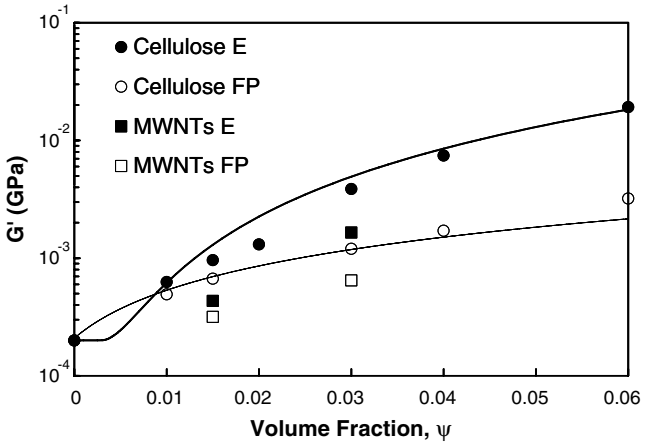

Fig. 8. Evolution of the nanocomposite shear storage modulus at $T/T_\alpha = 1.15$ with the filler content. Comparison with the one predicted by the mechanical percolation approach (——) and the one predicted by the mean field approach (—).

In order to understand this underestimation, it is worth considering the effect of this nanofibrils rigid network. An approach, called the mechanical percolation model, consists in the series-parallel model of Tagayanagi extended by Ouali et al. [31] and then by Kolařík [32] and Favier et al. [2] with a percolation concept. In this model, the composite is described by a parallel mechanical coupling of a rigid phase, made of a theoretical volume fraction of fiber network, and a soft one, made of the matrix reinforced with the fibers out of the network (i.e. dead branches and isolated aggregates). The network volume fraction is calculated from the percolation theory [33]. In the case of randomly distributed objects, the volume fraction P of percolated structure depends on the total volume fraction of objects, ψ, and is given by:

$$\begin{aligned} P(\psi) &= 0 && \text{for } \psi < \psi_c \\ P(\psi) &= \left(\frac{\psi-\psi_c}{1-\psi_c}\right)^b && \text{for } \psi \geqslant \psi_c \end{aligned} \quad (4)$$

with ψ_c, the percolation threshold and b, the critical exponent. As assumed by De Gennes [34], the dead branches do not participate actively in stress transmission. An account of only the backbone of the structure requires a value of b close to 1.8. The percolation threshold can be approximated to 0.23 vol% by using the law established by Nan [35] for straight rods, with an aspect ratio of 312 randomly dispersed in 3D. The shear modulus, G, of the composite is then given by:

$$G = \frac{(1-2P(\psi)+P(\psi)\psi)G_s G_r + (1-\psi)P(\psi)G_r^2}{(1-\psi)G_r + (\psi - P(\psi))G_s} \quad (5)$$

where G_r and G_s are, respectively, the shear moduli of the reinforcing phase (fiber percolating network) and of the soft one (the matrix). The modulus of the cellulose network, which obviously differs from that of isolated nanofibrils, can be estimated by measuring the elastic properties of a film made only of cellulose nanofibrils. The Young's modulus E_r was experimentally measured in tension and found to be 5 GPa. This value is close to the one reported by Dufresne et al. [36] (3 GPa on average) for sheets prepared from sugar beet cellulose. Assuming that the mechanical properties of nanofibrils sheets are isotropic, the shear modulus G_r can be calculated from E_r by taking a Poisson's ratio generally used for stiff systems ($v = 0.3$):

$$G_r = \frac{E_r}{2(1+v)} \quad (6)$$

The shear modulus values G' obtained from this percolation approach are found in Fig. 8 to be in good agreement with the mechanical measurements for E cellulose filled composites. For nanofibril volume fraction ψ lower than the percolation threshold ψ_c, nanofibrils get connected in small isolated aggregates, so that $P(\psi) = 0$ and the model is reduced to a series model which implies a low mechanical reinforcement. As soon as $\psi > \psi_c$, an "infinite" cluster begins to merge, a connected rigid cellulose network is

formed within the matrix, resulting in a jump of nanocomposite shear modulus.

Shear modulus values for MWNTs filled composites are also plotted in Fig. 8. These values appear very close to those of FP cellulose filled composites. Consequently, the mean field calculation seems adapted for MWNTs filled composites. As already mentioned before, no strong interactions are possible between carbon nanotubes, and thus a mechanical percolation phenomenon cannot occur. For instance, to model the modulus of the 3 vol% MWNTs filled E material in the glassy state, a filler longitudinal modulus of 300 GPa is required in the Halpin–Kardos isotropic calculation (Eq. (3)), almost independently on the aspect ratio. However, with the same fiber longitudinal modulus and an aspect ratio of 300, the mechanical reinforcement in the rubbery state is fitted. This value for the MWNTs longitudinal Young's modulus is lower than what is found in the literature (Demczyk and co-workers found for example by bending tests a longitudinal modulus of 910 GPa for MWNTs [10]). As it can be observed on Fig. 3, the carbon nanotubes remain curved and entangled within the composite. Fisher et al. [37] have shown by finite element calculation that the effective modulus of the tubes in composite materials is lower than their real longitudinal modulus and depends on their aspect ratio and their waviness ratio.

Nevertheless, the mean field approach alone cannot explain the fact that the nanotubes delay the flow of the material. Such a model does not take into account the mechanical interactions between fibers. Thus, the effect of entanglements between tubes is not taken into account.

In the case of conductive fillers, such as MWNTs, the investigation of the composite electrical percolation is of interest and could give information on the tube/tube contact properties in E and FP materials.

3.4. Electrical properties

Fig. 9 shows the evolution of the real part of the electrical conductivity with the frequency for carbon nanotubes filled materials. The P(S-BuA) matrix displays a classical dielectric material behavior, with an electrical conductivity increasing with the frequency for high values of frequency (>1 Hz). For the evaporated composite filled with 0.2 vol% the same type of behavior can be observed with a conductivity level higher than for the matrix and a dependency of the conductivity with the frequency which appears later (for $f > 10^4$ Hz). This composite displays a capacitive behavior which corresponds to a conductive filler/polymer composite really close to the percolation threshold. For higher nanotube contents (0.5 and 3 vol%), the composites electrical behavior is completely different, the conductivity is much higher (28 S m^{-1} for 3 vol% of MWNTs) and remains constant with the frequency: the materials exhibit purely real resistivity. In this case, the material is above the percolation threshold; there is a connective network of nanotubes within the matrix. The same type of results was obtained in the same range of conductivity value by

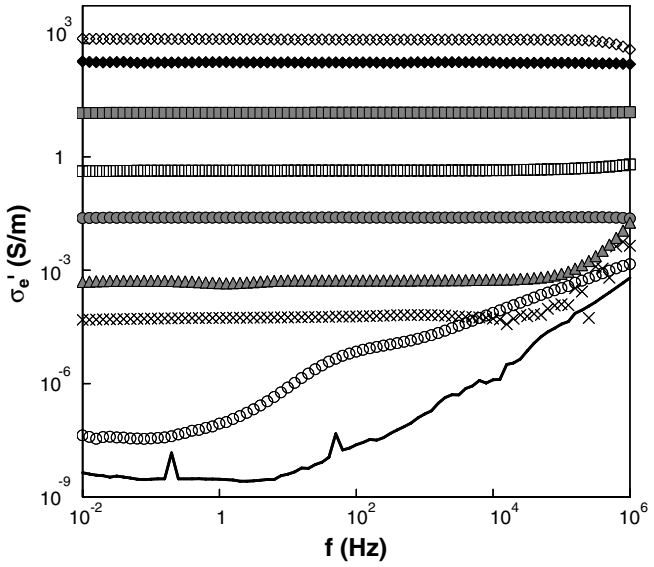

Fig. 9. Frequency dependence of the real part of the conductivity at room temperature for pure P(S-BuA) matrix (—), composites filled with 0.2 vol% (▲), 0.5 vol% (●) and 3 vol% (■) of MWNTs either E (gray filled symbols) or FP (unfilled symbols). Results for the SDBS surfactant (×), the SDBS/MWNTs film (♦) and the pure MWNTs (◊) are also plotted.

Sandler et al. [20] for epoxy/nanotubes composites or Benoit et al. [18] on PMMA/nanotubes composites. For FP materials, electrical conductivity level is systematically lower than for E materials and this transition from a capacitive behavior towards a resistive behavior appears for higher nanotube volume fraction. Indeed, the FP composite filled with 0.5 vol% of MWNTs displays a dielectric behavior really close to that of the pure matrix whereas the E one already displays high conductivity level with a resistive behavior.

The real part of the AC conductivity values at 1 Hz as a function of the nanotube content are plotted in Fig. 10. Statistical percolation theory [33,38] predicts a power law

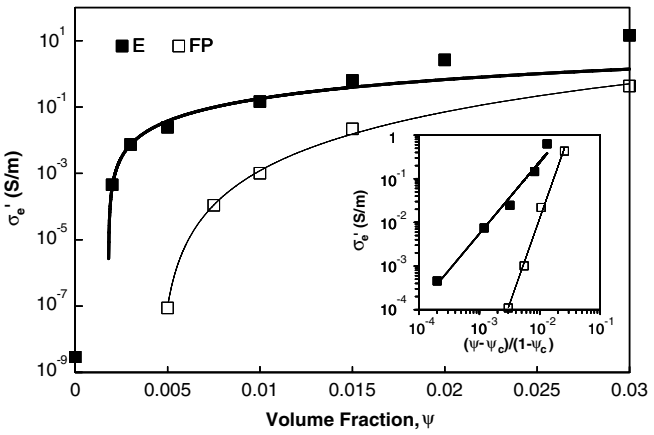

Fig. 10. Real part of the AC electrical conductivity at 1 Hz for different nanotubes contents in evaporated materials (E) and freeze-dried and pressed materials (FP). Comparison with predictions of statistical percolation theory (solid lines).

dependence for the conductivity above the percolation threshold:

$$\sigma_e \propto \left(\frac{\psi - \psi_c}{1 - \psi_c}\right)^t \quad (7)$$

where ψ is the MWNTs volume fraction, ψ_c the percolation threshold and t is the critical exponent for the conductivity. By using a linear fit on the log–log curve plotting the conductivity as a function of the reduced volume fraction $(\psi - \psi_c)/(1 - \psi_c)$, as shown in the inset of Fig. 10, the exponent t was found to be 1.7 and 3.9 for E and FP materials, respectively. Percolation thresholds ψ_c were adjusted to the values which give the best linear regression for ψ close to ψ_c. Thresholds of 0.18 vol% and 0.45 vol% were found for E and FP composites, respectively.

E materials present a classical percolation behavior of a system composed of high aspect ratio conductive fillers well-dispersed in an insulating matrix. Different numerical approaches found the same range for the critical exponent in conductivity of binary systems, between 1.7 and 2 in 3D [38–40]. Thus, the value of t obtained on E materials is consistent with this "universal" value. Low percolation thresholds were also found in other carbon nanotubes/polymer composites by Sandler et al. [20], Benoit et al. [18] or Regev et al. [21]. It confirms the good dispersion of very high aspect ratio conductive nanotubes in the polymer matrix. Indeed, as discussed by Nan [35], the percolation threshold is inversely proportional to the aspect ratio of the dispersed objects.

However, several numerical and experimental studies discussed the universality of the percolation critical exponent for conductivity properties [41–43]. Such theoretical studies demonstrated that in binary systems a distribution of the contact conductivity depending on the volume fraction of fillers (Balberg used tunneling conductance for example [41]) systematically leads to a critical exponent higher than the "universal" one. The lower conductivity level and the elevated value of t obtained for FP materials suggest that the freeze-drying process leads to a weaker electrical contact efficiency between carbon nanotubes. Indeed, as it was assumed previously with cellulose nanofibrils, the FP process leads to indirect contacts between nanotubes through matrix or surfactant, i.e. less conductive contacts. As supposed previously to explain DSC results, the FP process can certainly lead to a higher surfactant content in the composites. A part of this surfactant can be adsorbed on nanotube surface and is responsible for a weaker tube/tube contact electrical conductivity. Fig. 9 shows the low conductivity level of this surfactant (SDBS) and highlights its effect on the contact conductivity between nanotubes. Indeed, two films made of carbon nanotubes without polymer matrix were processed: one made by evaporation of raw MWNTs dispersed in ethanol, and the other from aqueous dispersion of MWNTs with SDBS. Both films are highly conductive but the use of surfactant (which has a an intermediate conductivity between that of the matrix and that of pure MWNTs as shown in Fig. 9) induces a weaker conductivity level (1300 S m^{-1} for pure MWNTS and 330 S m^{-1} MWNTs with SDBS). This is the result of the presence of surfactant at the contacts between nanotubes.

Moreover, in the FP systems, the contact conductivity may evolve with the nanotube volume fraction. Indeed, as discussed previously, the structure after the FP process is not relaxed, and the higher the nanotube content, the more constrained contacts between tubes. The contact electrical efficiency may thus increase with the nanotube content. Percolation theory were fitted for FP materials by using a percolation threshold more than two times higher than for E materials. Usually, the increase in percolation threshold is related to changes in the microstructure. This is consistent with the assumption made in Fig. 6. Indeed, the FP process leads to a nanotube structure which is not completely relaxed, thus they could remain more tortuous than in the E composites. Such nanotubes with higher tortuosity can be compared to equivalent fillers with a lower aspect ratio, inducing a higher percolation threshold. A discrete modeling approach taking into account the morphology of such nanotube filled nanocomposites and the electrical properties of the tubes themselves and of the tube–tube contacts were developed to discuss this influence of the processing conditions on the electrical percolation. This study is presented in another article [44].

4. Conclusion

High aspect ratio nanofibers/P(S-BuA) composites were elaborated with two different processing conditions. Such fillers present good flexibility properties that can induce the formation of an entangled fiber network within the composite above a critical fibers volume fraction (which can be interpreted as a geometrical percolation threshold). By studying two different types of nano-fillers with two processing routes, this work highlighted two essential effects on such entangled structures: the influence of fiber entanglements on composite thermo-mechanical behavior and the importance of fiber/fiber contact efficiency on the composite macroscopic properties. Different assumptions were made to explain the influence of processing conditions on composite electrical and mechanical properties in the rubbery state. We summarized them here for the four different systems in descending order of the resulting mechanical reinforcement:

(i) E cellulose filled composites: Formation of a rigid nanofibril network linked by strong hydrogen bonds. Such contacts, where stress transfer is possible, lead to the highest mechanical reinforcement (with a mechanical percolation phenomenon) coupled to an increase in composites thermo-mechanical stability.
(ii) FP cellulose filled composites: The FP process prevents the creation of strong contacts between nanofibrils. A lower mechanical reinforcement is measured; the increase in modulus is only due to the stress transfer between the matrix and the fibrils (mechanical

percolation with a strong increase of the modulus does not occur). Interactions between nanofibrils and polymer chains lead to an increase in the flow temperature.

(iii) E MWNTs filled composites: The formation of an entangled network is responsible for the strong increase in thermo-mechanical stability (a large rubbery plateau is observed). As strong interactions between nanotubes are impossible, a relatively low mechanical reinforcement is obtained and is well modeled by a classical mean field approach. The existence of this percolating MWNT network is detectable via the material electrical properties where a percolation phenomenon is measured.

(iv) FP MWNTs filled composites: The FP process prevents the entanglement formation between nanotubes. This implies a lower flow temperature of the composites but with almost the same mechanical reinforcement measured at room temperature (entanglements do not seem to play a role on mechanical reinforcement). Moreover, contact electrical properties are weaker (an assumption is made of a higher adsorbed surfactant amount in the case of freeze-dried materials) leading to changes in the electrical percolation.

As a conclusion, two main effects were differentiated in this study: the effect of fiber entanglements on thermo-mechanical properties and the effect of the contact strength on the mechanical reinforcement level.

Acknowledgements

The authors thank C. Graillat (LCPP, CPE Lyon, France) for his help and his fruitful advises in latex synthesis as well as I. Paintrand and M-F Marais (CERMAV, Grenoble, France) for their help in cellulose processing and characterization. They also acknowledge K. Masenelli-Varlot (GEMPPM, INSA Lyon, France) for the preparation of TEM sample microsections; and E. Couteau and A. Magrez (IPCM, EPFL, Switzerland) for the preparation of carbon nanotubes. The work in Lausanne was supported by the Swiss National Science Foundation and its NCCR "Nanoscale Science. This work was performed in the frame of the European CNT-network and the GDRE No. 2756 "Science and applications of the nanotubes – NANO-E".

References

[1] Chazeau L, Gauthier C, Vigier G, Cavaillé JY. Relashionships between microstructural aspects and mechanical properties of polymer-based nanocomposites. Handbook of organic–inorganic hybrid materials and nanocomposites, vol. 2. Los Angles: American Scientific Publishers; 2003.

[2] Favier V, Canova G, Shrivastava S, Cavaillé JY. Mechanical percolation in cellulose whisker nanocomposites. Polym Eng Sci 1997;37(10):1732–9.

[3] Favier V, Dendievel R, Canova G, Cavaillé JY, Gilormini P. Simulation and modeling of three-dimensional percolation structures: case of latex matrix reinforced by a network of cellulose fibers. Acta Mater 1997;45(4):1557–65.

[4] Neville AC. Biology of fibrous composites. New York: Cambridge University Press; 1993.

[5] Eichhorn SJ, Young RJ. The Young's modulus of microcrystalline cellulose. Cellulose 2001;8:197–207.

[6] Dinand E, Chanzy H, Vignon MR. Parenchymal cell cellulose from sugar beet pulp: preparation and properties. Cellulose 1996;3:183–8.

[7] Orts WJ, Shey J, Imam SH, Glenn GM, Guttman ME, Revol JF. Application of cellulose microfibrils in polymer nanocomposites. J Polym Environ 2005;13(4):301–6.

[8] Dufresne A, Vignon MR. Improvement of starch film performances using cellulose microfibrils. Macromolecules 1998;31(8):2693–6.

[9] Ijima S. Helical microtubules of graphitic carbon. Nature 1991;354:56–8.

[10] Demczyk BG, Wang YM, Cumings J, Hetman M, Han W, Zettl A, et al. Direct mechanical measurement of the tensile strength and elastic modulus of multiwalled carbon nanotubes. Mater Sci Eng A 2002;334:173–8.

[11] Nardelli MB, Fattebert JL, Orlikowski D, Roland C, Zhao Q, Bernholc J. Mechanical properties, defects and electronic behavior of carbon nanotubes. Carbon 2000;38:1703–11.

[12] Jia Z, Wang Z, Xu C, Liang J, Wei B, Wu D, et al. Study on poly(methyl methacrylate)/carbon nanotube composites. Mater Sci Eng A 1999;271:395–400.

[13] Cooper CA, Ravich D, Lips D, Mayer J, Wagner HD. Distribution and alignment of carbon nanotubes and nanofibrils in a polymer matrix. Comp Sci Technol 2002;62:1105–12.

[14] Pötschke P, Fornes TD, Paul DR. Rheological behavior of multiwalled carbon nanotube/polycarbonate composites. Polymer 2002;43:3247–55.

[15] Thostenson ET, Ren Z, Chou TW. Advances in the science and technology of carbon nanotubes and their composites: a review. Comp Sci Technol 2001;61:1899–912.

[16] Velasco-Santos C, Martínez-Hernández AL, Fisher F, Ruoff R, Castaño VM. Dynamical-mechanical and thermal analysis of carbon nanotube-methyl–ethyl methacrylate nanocomposites. J Phys D: Appl Phys 2003;36:1423–8.

[17] Kaneto K, Tsuruta M, Sakai G, Cho WY, Ando Y. Electrical conductivities of multi-wall carbon nanotubes. Synthetic Met 1999;103:2543–6.

[18] Benoit JM, Corraze B, Lefrant S, Blau WJ, Bernier P, Chauvet O. Transport properties of PMMA-carbon nanotubes composites. Synthetic Met 2001;121:1215–6.

[19] Kilbride BE, Coleman JN, Fraysse J, Fournet P, Cadek M, Drury A, et al. Experimental observation of scaling laws for alternating current and direct current conductivity in polymer-carbon nanotube composite thin films. J Appl Phys 2002;92(7):4024–30.

[20] Sandler JKW, Kirk JE, Kinloch IA, Shaffer MSP, Windle AH. Ultra-low electrical percolation threshold in carbon-nanotube-epoxy composites. Polymer 2003;44:5893–9.

[21] Regev O, ElKati PNB, Loos J, Koning CE. Preparation of conductive nanotube-polymer composites using latex technology. Adv Mater 2004;16(3):248–51.

[22] Couteau E, Hernadi H, Seo JW, Thiên-Nga L, Miko C, Gaal R, et al. CVD synthesis of high purity multiwalled carbon nanotubes using $CaCO_3$ catalyst support for large-scale production. Chem Phys Lett 2003;378:9–17.

[23] Bogner A, Thollet G, Basset D, Jouneau PH, Gauthier C. Wet STEM: a new development in environmental SEM for imaging of nano-objects included in a liquid phase. Ultramicroscopy 2005;104:290–301.

[24] Steward PA, Hearn J, Wilkinson MC. An overview of polymer latex film formation and properties. Adv Colloid Interface Sci 2000;86:195–267.

[25] Belaroui F, Hirn MP, Grohens Y, Marie P, Holl Y. Distribution of water-soluble and surface-active low-molecular-weight species in acrylic latex films. J Colloid Interface Sci 2003;261:336–48.

[26] Halpin JC. Stiffness and expansion estimates for oriented short fiber composites. J Compos Mater 1969;3:732–4.
[27] Berthelot JM. Matériaux composites-Comportement mécanique et analyse des structures, Masson.
[28] Van Es MA. Polymer–clay nanocomposites: the importance of particle dimensions. PhD Thesis, Technische Universiteit Delft, 2001.
[29] Eichhorn SJ, Baillie CA, Zafeiropoulos N, Mwaikambo LY, Ansell MP, Dufresne A, et al. Review: Current international research into cellulosic fibres and composites. J Mater Sci 2001;36:2107–31.
[30] Dinand E. Microfibrilles de cellulose: isolement a partir de pulpes de betterave, caractérisation et propriétés. PhD Thesis, Université Joseph Fourier, Grenoble, 1997.
[31] Ouali N, Cavaillé JY, Perez J. Elastic, viscoelastic and plastic behavior of multiphase polymer blends. Plast Rubber Compos Process Appl 1991;16:55–60.
[32] Kolarik J. Simultaneous prediction of the modulus, tensile strength and gas permeability of binary polymer blends. Eur Polym J 1997;34(5/6):585–90.
[33] Gouyet JF. Physique et structures fractales. Paris: Masson; 1992.
[34] De Gennes PG. On the relation between percolation theory and the elasticity of gels. J Phys Lett 1976;37:L1–2.
[35] Nan CW. Physics of inhomogeneous inorganic materials. Prog Mater Sci 1993;37:1–116.
[36] Dufresne A, Cavaillé JY, Vignon MR. Mechanical behavior of sheets prepared from sugar beet cellulose microfibrils. J Appl Polym Sci 1997;64:1185–94.
[37] Fisher FT, Bradshaw RD, Brinson LC. Fiber waviness in nanotube-reinforced polymer composites – I: modulus predictions using effective nanotube properties. Comp Sci Technol 2003;63:1689–703.
[38] Kirkpatrick S. Percolation and conduction. Rev Mod Phys 1973;45(4):574–88.
[39] Balberg I, Binenbaum N. Computer study of the percolation threshold in a two-dimensional anisotropic system of conducting sticks. Phys Rev B 1983;28(7):3799–812.
[40] Pike GE, Seager CH. Percolation and conductivity: a computer study. Phys Rev B 1974;10(4):1421–34.
[41] Balberg I. Tunneling and nonuniversal conductivity in composite materials. Phys Rev Lett 1987;59(12):1305–8.
[42] Halperin BI, Feng S, Sen PN. Differences between lattice and continuum percolation transport exponents. Phys Rev Lett 1985;54(22):2391–4.
[43] Heaney MB. Measurement and interpretation of nonuniversal critical exponents in disordered conductor–insulator composites. Phys Rev B 1995;52(17):12477–80.
[44] Dalmas F, Dendievel R, Chazeau L, Cavaillé JY, Gauthier C. Carbon nanotube filled polymer composites: numerical simulation of electrical conductivity in three dimensional entangled fibrous networks. Acta Mat 2006;54(11):2709–18.